LETTER

# Observing quantum control of up-conversion luminescence in $Dy^{3+}$ ion doped glass from weak to intermediate shaped femtosecond laser fields

IOP Publishing | Astro Ltd
Laser Physics Letters
Laser Phys. Lett. **14** (2017) 115301 (7pp)
https://doi.org/10.1088/1612-202X/aa877b

## Letter

# Observing quantum control of up-conversion luminescence in $Dy^{3+}$ ion doped glass from weak to intermediate shaped femtosecond laser fields

**Pei Liu[1], Wenjing Cheng[2], Yunhua Yao[1], Cheng Xu[3], Ye Zheng[1], Lianzhong Deng[1], Tianqing Jia[1], Jianrong Qiu[3], Zhenrong Sun[1] and Shian Zhang[1,4]**

[1] State Key Laboratory of Precision Spectroscopy, East China Normal University, Shanghai 200062, People's Republic of China
[2] School of Physics and Electrical Information, Shangqiu Normal University, Shangqiu 476000, People's Republic of China
[3] State key Laboratory of Silicon Materials, Zhejiang University, Hangzhou 310027, People's Republic of China
[4] Collaborative Innovation Center of Extreme Optics, Shanxi University, Taiyuan, Shanxi 030006, People's Republic of China

E-mail: 0110wenjing@163.com and sazhang@phy.ecnu.edu.cn

Received 13 April 2017, revised 14 August 2017
Accepted for publication 14 August 2017
Published 26 October 2017


**Abstract**

Controlling the up-conversion luminescence of rare-earth ions in real-time, in a dynamical and reversible manner, is very important for their application in laser sources, fiber-optic communications, light-emitting diodes, color displays and biological systems. In previous studies, the up-conversion luminescence control mainly focused on the weak femtosecond laser field. Here, we further extend this control behavior from weak to intermediate femtosecond laser fields. In this work, we experimentally and theoretically demonstrate that the up-conversion luminescence in $Dy^{3+}$ ion doped glass can be artificially controlled by a $\pi$ phase step modulation, but the up-conversion luminescence control behavior will be affected by the femtosecond laser intensity, and the up-conversion luminescence is suppressed by lower laser intensity while enhanced by higher laser intensity. We establish a new theoretical model (i.e. the fourth-order perturbation theory) to explain the physical control mechanism by considering the two- and four-photon absorption processes, and the theoretical results show that the relative weight of four-photon absorption in the whole excitation process will increase with the increase in laser intensity, and the interference between two- and four-photon absorptions results in up-conversion luminescence control modulation under different laser intensities. These theoretical and experimental works can provide a new method to control and understand up-conversion luminescence in rare-earth ions, and also may open a new opportunity to the related application areas of rare-earth ions.

Keywords: up-conversion luminescence, quantum control, pulse shaping, rare-earth ions

(Some figures may appear in colour only in the online journal)

 

## 1. Introduction

The up-conversion luminescence of rare-earth ions can generate radiation light that has a shorter wavelength than the pump light through two-photon or multi-photon absorption processes, and therefore the up-conversion luminescence of rare-earth ion doped luminescent materials has attracted considerable attention because of its excellent optical properties, such as photo-stability, narrow spectrum, near infrared excitation, large Stokes shift, long luminescence lifetime and well-defined emission bands [1, 2]. So far, rare-earth ion doped luminescent materials have been widely applied in some related areas, such as laser sources [3, 4], fiber-optic communications [5, 6], light-emitting diodes [7], solar cells [8], color displays [9, 10], biolabeling and biomedical sensing [11–15], and so on. In the up-conversion excitation technique, a near-infrared (NIR) laser was usually used as the excitation source due to its deeper penetration depth in the sample than that obtained using an ultraviolet laser. Moreover, using the NIR laser can significantly minimize background autofluorescence, photobleaching and photodamage.

How to control the up-conversion luminescence of rare-earth ions has become a hot research topic in various related areas of rare-earth ions. Realizing the tuning or enhancement of the up-conversion luminescence in rare-earth ions is an essential request for optimizing the performance and processes of optical devices, and is also important fundamental research for understanding up-conversion luminescence mechanisms and multi-photon excitation processes [16]. Usually, there are two main methods for controlling the up-conversion fluorescence of rare-earth ions. One is the conventional chemical method, which is a very effective technique to tune or enhance the up-conversion luminescence of rare-earth ions, such as changing chemical composition [2, 17], crystal structure [18], nanoparticle size [19], and surface groups [20]. However, the conventional chemical method cannot control the up-conversion luminescence in a real-time, dynamical and reversible manner. The other one is the physical method, such as applying an electric field [21], magnetic field [22], plasmon [23], or temperature [24], or changing the laser wavelength [25], laser pulse duration [26], or laser repetition [27]. Recently, we proposed a femtosecond pulse shaping technique to tune, suppress or enhance the up-conversion luminescence of rare-earth ions, and obtained a series of research results [28–32]. For example, the single- and two-photon fluorescence in $Er^{3+}$ ions can be enhanced or suppressed by a $\pi$ or square phase modulation [28, 29]; the up-conversion fluorescence in $Er^{3+}$ or $Dy^{3+}$ ions can be effectively controlled by varying both the laser polarization or phase [30, 31]; The green and red up-conversion fluorescence can be tuned in $Er^{3+}$-doped $NaYF_4$ nanocrystals by square phase modulation [32].

Our previous works focused on the quantum coherent control of up-conversion luminescence in rare-earth ions under a weak shaped femtosecond laser field [28–32]. In this paper, we experimentally and theoretically observe the up-conversion luminescence control behavior in $Dy^{3+}$ ion doped glass from weak to intermediate shaped femtosecond laser fields. Our experimental results show that the up-conversion luminescence can be effectively controlled by a $\pi$ phase modulation under both lower and higher laser intensity excitations, but the up-conversion luminescence control behavior is correlated with the femtosecond laser intensity, which is suppressed under lower laser intensity excitation while it is enhanced under higher laser intensity excitation. Our theoretical simulations demonstrate that the experimental observations can be well explained by using a fourth-order perturbation theory, which involves the two- and four-photon absorption processes. With the increase in the laser intensity, the relative weight of the four-photon absorption in the whole excitation process will increase, and the interference between two- and four-photon excitation pathways results in different up-conversion luminescence control behaviors under lower and higher laser intensities.

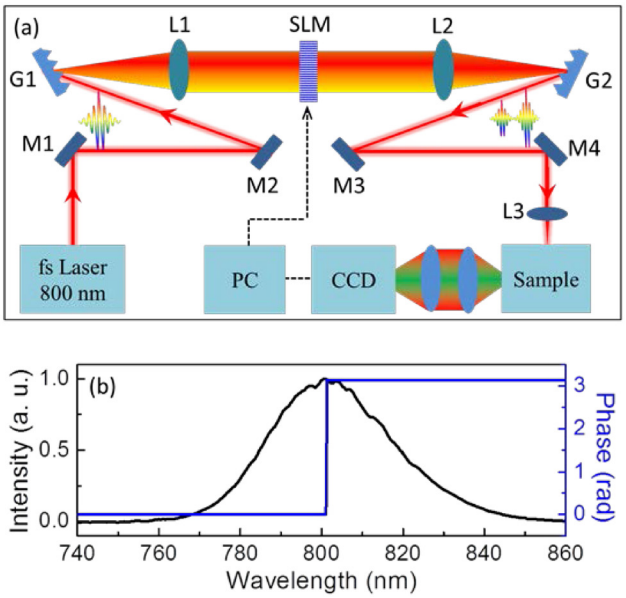


**Figure 1.** (a) The experimental arrangement for the control of up-conversion luminescence in a $Dy^{3+}$-doped glass sample using a shaped femtosecond laser pulse. Here, the zero-dispersion programmable 4f-configuration femtosecond pulse shaping system includes a pair of gratings, a pair of lenses and a spatial light modulator (SLM); here the SLM is placed at the Fourier plane and used to control the spectral phase and amplitude in the frequency domain. (b) The femtosecond laser spectrum is modulated by a $\pi$ phase step modulation.

## 2. Experimental arrangement

Our experimental arrangement is shown in figure 1(a). Here, a Ti-sapphire femtosecond laser (Spectra-physics, Spitfire) is used as the excitation source with a central wavelength of 800 nm, repetition rate of 1 kHz and pulse width of about 50 fs. The output femtosecond laser pulse is shaped by using a zero-dispersion programmable 4-f configuration pulse shaping system. The femtosecond pulse shaping system is composed of a pair of diffraction gratings with 1200 lines $mm^{-1}$ (G1 and G2), a pair of concave mirrors with focal length of 200 mm (L1 and L2) and a one-dimension liquid crystal spatial light modulator array (SLM-S320d, JENOPTIK). Here, the SLM is placed at the Fourier plane and used to control the spectral

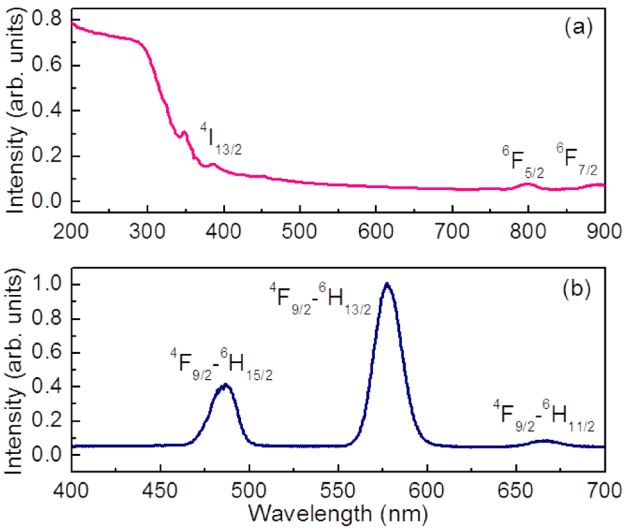


**Figure 2.** (a) The UV–vis–NIR absorption spectrum of a $Dy^{3+}$-doped glass sample. (b) The up-conversion luminescence spectrum in the visible light region under 800 nm femtosecond laser pulse excitation.

phase or amplitude in the frequency domain. By approximately designing the spectral phase and/or amplitude, such a shaped femtosecond laser pulse with almost arbitrary temporal distribution can be obtained. The shaped femtosecond laser pulse is focused into the $Dy^{3+}$ ion doped glass sample through a lens of 50 mm focal length. All the up-conversion luminescence signals emitted from the $Dy^{3+}$ ion doped glass sample are perpendicularly collected and measured by a spectrometer with a charge-coupled device (CCD). In order to obtain the stable spectral signals, here the measured luminescence spectra in our experiments are all averaged five times.

In our experiment, the sample is a piece of glass doped with $Dy^{3+}$ ions, which is synthesized via optimal modification from melt quenching to subsequent heat treatment. During the glass sample preparation, a 4N rare earth compound ($Dy_2O_3$) is used as raw material. The precursor sample doped with $Dy^{3+}$ ions is synthesized with the composition (in mol%) of 60%$SiO_2$, 20%$Al_2O_3$, 20%$CaF_2$ and 1%$DyF_3$. A platinum crucible with a lid is used to melt the mixed raw materials, which are treated for 45 min at 1450 °C in ambient atmosphere, and then molded in a brass mould followed by a 10 h anneal at 450 °C. Finally, the glass products are further processed through incision and polishing, and are used in our optical measurement.

## 3. Results and discussion

The UV–vis–NIR absorption spectrum of the $Dy^{3+}$-doped glass sample is shown in figure 2(a), which is measured using a U-4100 spectrophotometer (Hitachi). It can be seen that three main absorption bands are observed around the wavelengths of 388, 800 and 891 nm, which correspond to the three excited states $^4I_{13/2}$, $^6F_{5/2}$ and $^6F_{7/2}$. In our experiment, the up-conversion luminescence spectrum under the 800 nm femtosecond laser pulse excitation in the visible light region is shown in figure 2(b). One can see that three up-conversion luminescence signals can be clearly observed around the wavelengths of 487, 577 and 665 nm, which can be attributed to the three state transitions $^4F_{9/2} \rightarrow {}^6H_{15/2}$, $^4F_{9/2} \rightarrow {}^6H_{13/2}$ and $^4F_{9/2} \rightarrow {}^6H_{11/2}$, respectively. The same experiment is also performed in the glass sample without $Dy^{3+}$ ions, and no up-conversion luminescence signal can be observed. This phenomenon confirms that the up-conversion luminescence in figure 2(a) comes from the excitation of $Dy^{3+}$ ions. Here, the $\pi$ phase step modulation is used to control the up-conversion luminescence, which is featured with a phase jump within the femtosecond laser spectrum from 0 to $\pi$ at a certain phase step position, as shown in figure 1(b). The $\pi$ phase step modulation is regarded as a well-established tool for inducing constructive or destructive interference between different excitation pathways, and therefore has been extensively applied in atomic and molecular systems to control the multi-photon absorption process [33, 34].

Figure 3 presents the normalized up-conversion luminescence intensity at a wavelength of 577 nm by varying the $\pi$ phase step modulation with the laser intensities of $4.9 \times 10^{12}$ (a), $9.8 \times 10^{12}$ (b), $2.45 \times 10^{13}$ (c) and $4.9 \times 10^{13}$ W cm$^{-2}$ (d), together with the theoretical simulations. Here, the laser average power is measured by a OPHIR power meter (Newport), and the laser intensity (i.e. peak power) is calculated using the formula $I = P/(\tau \times \gamma \times \sigma)$, where $P$ is the average power, $\tau$ is the laser pulse width, $\gamma$ is the laser repetition rate, and $\sigma$ is the laser spot size. For convenience, we use the up-conversion luminescence signal at the wavelength of 577 nm as our study object, and the other two up-conversion luminescence signals have the same control behavior. As can be seen, the up-conversion fluorescence can be controlled in a real-time, dynamical and reversible manner by $\pi$ phase step modulation. More importantly, the up-conversion luminescence intensity can be effectively suppressed or enhanced, which depends on the femtosecond laser intensity. That is to say, one can artificially control the up-conversion luminescence suppression or enhancement of the $Dy^{3+}$-doped glass sample according to the experimental requirement. With the increase in the laser intensity, the up-conversion luminescence control behavior is from suppression to enhancement. The up-conversion fluorescence can be suppressed but not enhanced with lower laser intensity (see figure 3(a)), while it can be enhanced but not suppressed with higher laser intensity (see figure 3(d)).

To explain why the $\pi$ phase step modulation can control the up-conversion luminescence suppression or enhancement under the different laser intensities, we theoretically consider the two- and four-photon absorption processes in the $Dy^{3+}$ ions, as show in figure 4. Here, the three states $^6H_{15/2}$, $^6F_{5/2}$ and $^4I_{13/2}$ represent the ground state $|g\rangle$, intermediate state $|i\rangle$ and final excited state $|f\rangle$, respectively. In the two-photon absorption process, the initial population in the ground state $^6H_{15/2}$ is pumped to the final excited state $^4I_{13/2}$ via the intermediate state $^6F_{5/2}$ by absorbing two photons (i.e. resonance-mediated two-photon absorption). In the four-photon absorption process, the state transition includes both the contributions from the resonance Raman part via the intermediate state $^6F_{5/2}$ or the ground state

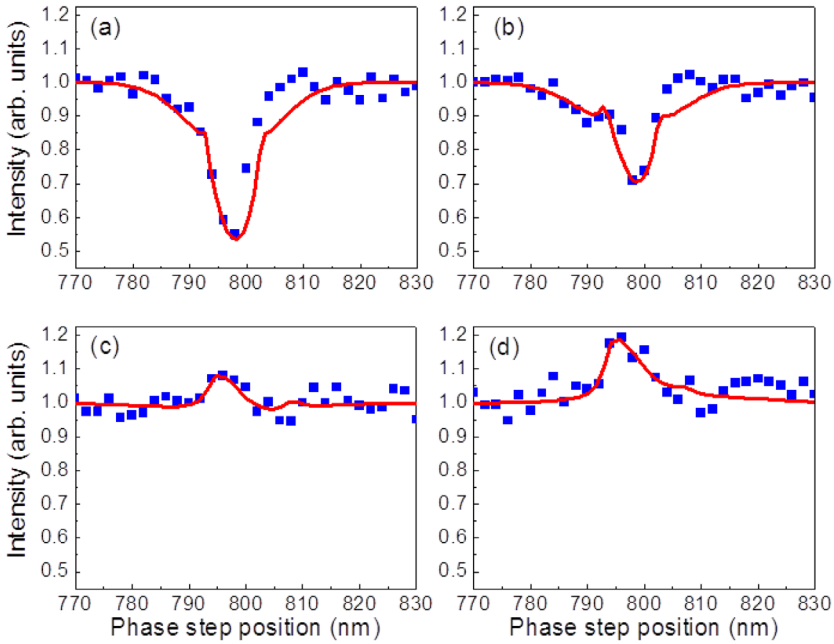


**Figure 3.** The normalized up-conversion luminescence intensity at a wavelength of 577 nm with varying the $\pi$ phase step position with the laser intensities of $4.9 \times 10^{12}$ (a), $9.8 \times 10^{12}$ (b), $2.45 \times 10^{13}$ (c) and $4.9 \times 10^{13}$ W cm$^{-2}$ (d).

$^6H_{15/2}$, and the non-resonant Raman part via the virtual state $|n\rangle$. The population in the final excited state $^4I_{13/2}$ will relax to the lower excited state $^4F_{9/2}$, and emits the up-conversion fluorescence at these wavelengths of 487, 577 and 665 nm via the three state transitions of $^4F_{9/2} \rightarrow {}^6H_{15/2}$, $^4F_{9/2} \rightarrow {}^6H_{13/2}$ and $^4F_{9/2} \rightarrow {}^6H_{11/2}$, respectively. Usually, the multi-photon absorption in the quantum system with the broadband absorption can be considered as the sum of each individual transition pathway [34]. Therefore, the population in the final excited state $^4I_{13/2}$ (i.e. $|f\rangle$) can be written as [35, 36]

$$P_f \propto \int_{-\infty}^{\infty} A_{\mathrm{abs}}(\omega_{fg}) |A_f(\omega_{fg})|^2 \mathrm{d}\omega_{fg}, \tag{1}$$

with

$$A_f(\omega_{fg}) = A_f^{(2)} + A_f^{(4)}. \tag{2}$$

One can see that the final state amplitude $A_f(\omega_{fg})$ involves both the contributions from the second- and fourth-order perturbation terms, i.e. $A_f^{(2)}$ and $A_f^{(4)}$. The second-order term $A_f^{(2)}$ includes all the two-photon excitation pathways, and can be described as [33]

$$A_f^{(2)} = -\frac{1}{\mathrm{i}\hbar^2} |E_0|^2 A^{(2)}(\omega_{fg}), \tag{3}$$

with

$$A^{(2)}(\Omega) = \mu_{fi}\mu_{ig} \int_{-\infty}^{\infty} \mathrm{d}\omega_{ig} \left[ \mathrm{i}\pi A_{\mathrm{abs}}(\omega_{ig}) \hat{E}(\omega_{ig}) \hat{E}(\Omega - \omega_{ig}) + \wp \int_{-\infty}^{\infty} \mathrm{d}\omega \hat{E}(\omega) \hat{E}(\Omega - \omega) / (\omega_{ig} - \omega) \right]. \tag{4}$$

However, the fourth-order term $A_f^{(4)}$ interferes with all the four-photon excitation pathways with three absorbed photons and one emitted photon, and is given by [37–39]

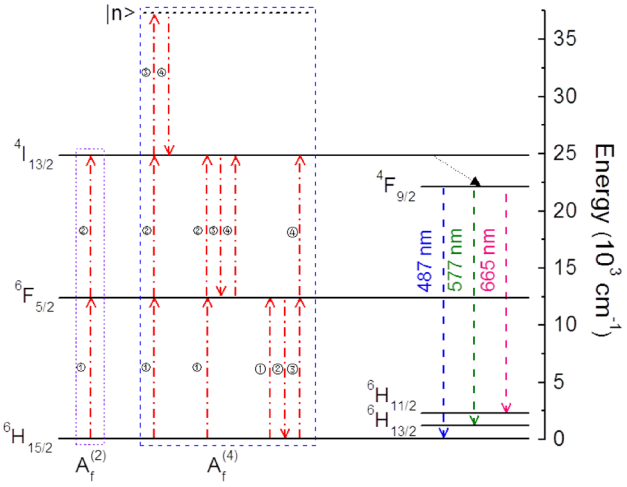


**Figure 4.** The energy level diagram of $Dy^{3+}$ ion and possible up-conversion excitation processes by two- and four-photon absorptions.

$$A_f^{(4)} = -\frac{1}{\mathrm{i}\hbar^4} |E_0|^4 \left[ \mathrm{i}\pi A^{(2)}(\omega_{fg}) A^{(\mathrm{R})}(0) - \wp \int_{-\infty}^{\infty} \mathrm{d}\delta A^{(2)}(\omega_{fg} - \delta) A^{(\mathrm{R})}(\delta)/\delta \right], \tag{5}$$

where $A^{(R)}(\delta)$ can be defined as

$$A^{(\mathrm{R})}(\Delta\Omega) = A_{fi}^{(\mathrm{resR})}(\Delta\Omega) + A_{ig}^{(\mathrm{resR})}(\Delta\Omega) + A_n^{(\mathrm{non\text{-}resR})}(\Delta\Omega), \tag{6}$$

with

$$A_{fi}^{(\mathrm{resR})}(\Delta\Omega) = |\mu_{fi}|^2 \left[ \mathrm{i}\pi \hat{E}(\omega_{fi}) \hat{E}^*(\omega_{fi} - \Delta\Omega) - \wp \int_{-\infty}^{\infty} \mathrm{d}\delta' \hat{E}(\omega_{fi} - \delta') \hat{E}^*(\omega_{fi} - \Delta\Omega - \delta')/\delta' \right], \tag{7}$$

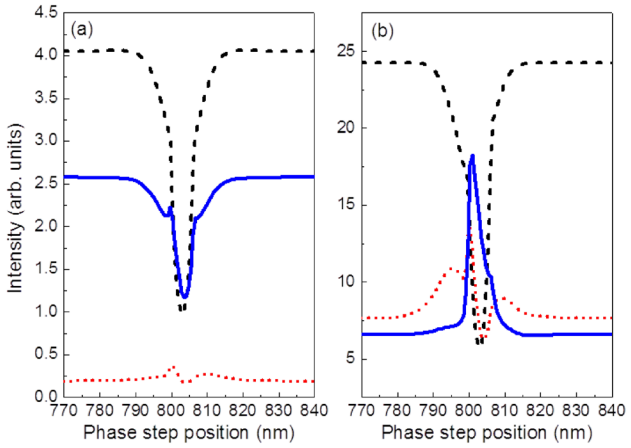


**Figure 5.** The theoretical simulation of $^4I_{13/2}$ state absorption with varying the $\pi$ phase step position with a lower laser intensity of $2 \times 10^{12}$ W cm$^{-2}$ (a) and higher laser intensity $8 \times 10^{13}$ W cm$^{-2}$ (b), together with the contributions of two- (black dashed line) and four-photon absorption (red dotted line).

$$A_{ig}^{(\mathrm{resR})}(\Delta\Omega) = |\mu_{ig}|^2 \left[ \mathrm{i}\pi \hat{E}(\omega_{ig})\hat{E}^*(\omega_{ig} - \Delta\Omega) - \wp \int_{-\infty}^{\infty} \mathrm{d}\delta' \hat{E}(\omega_{ig} - \delta')\hat{E}^*(\omega_{ig} - \Delta\Omega - \delta')/\delta' \right], \quad (8)$$

$$A_n^{(\mathrm{non\text{-}resR})}(\Delta\Omega) = \mu_{nn}^2 \int_{-\infty}^{\infty} \hat{E}(\omega + \Delta\Omega)\hat{E}^*(\omega)\mathrm{d}\omega, \quad (9)$$

where $A_{\mathrm{abs}}(\omega_{ig})$ and $A_{\mathrm{abs}}(\omega_{fg})$ are the absorption line-shape functions of the intermediate state $|i\rangle$ (i.e. $^6F_{5/2}$) and final excited state $|f\rangle$ (i.e. $^4I_{13/2}$), $\wp$ is the Cauchy principal value, $\omega_{ig}$, $\omega_{fi}$ and $\omega_{fg}$ are the transition frequencies of $|g\rangle \rightarrow |i\rangle$, $|i\rangle \rightarrow |f\rangle$ and $|g\rangle \rightarrow |f\rangle$, $\mu_{fi}$ and $\mu_{ig}$ are the dipole moment matrix elements, and $\mu_{nn}^2$ is the effective non-resonant Raman coupling via the virtual state $|n\rangle$. The spectral field is written as $E(\omega) = |E(\omega)|\exp[\mathrm{i}\phi(\omega)]$, where $E(\omega)$ and $\phi(\omega)$ are the spectral amplitude and phase at the frequency $\omega$. Here, we use the normalized spectral field $\hat{E}(\omega) = |E(\omega)|/|E_0|$ to represent the laser field shape, and $E_0$ is the maximal spectral amplitude. Based on our theoretical model, we theoretically simulate the population in the final state $^4I_{13/2}$ (i.e. $|f\rangle$) $P_f$ according to our experimental conditions, and the simulated results are also shown in figure 3. Obviously, the theoretical simulations can be in good agreement with the experimental results, which illustrates the important role of four-photon absorption on the up-conversion luminescence control under the higher laser intensity. Furthermore, these theoretical results also show that the interference between the two- and four-photon excitation pathways results in different up-conversion luminescence control behaviors under lower and higher laser intensities.

In order to further illustrate the physical control mechanism of the up-conversion luminescence suppression or enhancement, we present the theoretical results of the $^4I_{13/2}$ state absorption by varying the $\pi$ phase step position with the lower laser intensity of $2 \times 10^{12}$ W cm$^{-2}$ (a) and the higher laser intensity of $8 \times 10^{13}$ W cm$^{-2}$ (b), together with the contributions of two- (black dashed line) and four-photon absorption (red dotted line) (i.e. $|A_f^{(2)}|^2$ and $|A_f^{(4)}|^2$), as shown in figure 5. One can see that the two-photon absorption $|A_f^{(2)}|^2$ can be suppressed but not enhanced by $\pi$ phase modulation under both the lower and higher laser intensities, while the four-photon absorption $|A_f^{(4)}|^2$ can be enhanced or suppressed. Furthermore, it can be seen from equations (3) and (5) that the second-order term $A_f^{(2)}$ is proportional to $|E_0|^2$, while the fourth-order term $A_f^{(4)}$ is proportional to $|E_0|^4$. Consequently, the two-photon absorption $|A_f^{(2)}|^2$ is far larger than the four-photon absorption $|A_f^{(4)}|^2$ under the lower laser intensity, and therefore plays the main role for the up-conversion luminescence; thus the up-conversion luminescence cannot be enhanced, as shown in figure 5(a). However, the four-photon absorption contribution $|A_f^{(4)}|^2$ can be compared with the two-photon absorption contribution $|A_f^{(2)}|^2$ under higher laser intensity; the constructive interference between the two- and four-photon excitation pathways results in up-conversion luminescence enhancement, as shown in figure 5(b). Obviously, the four-photon absorption contribution plays a crucial role in the up-conversion luminescence enhancement, and therefore one can select an appropriate laser intensity to modulate the up-conversion luminescence control behavior by the $\pi$ phase step modulation.

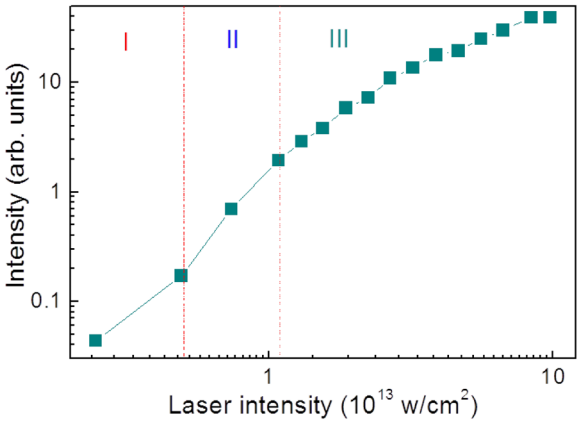


**Figure 6.** The up-conversion luminescence intensity at a wavelength of 577 nm with varying the femtosecond laser intensity.

In order to confirm the four-photon absorption contribution under the higher laser intensity, we measure the up-conversion luminescence intensity at the wavelength of 577 nm by varying the femtosecond laser intensity, and the log–log plot of the luminescence intensity versus the laser intensity is shown in figure 6. In the lower laser intensity region (i.e. region I), the slope is relatively small, which illustrates that the up-conversion luminescence mainly comes from the two-photon absorption contribution. However, in the higher laser intensity region (i.e. region II), the slope quickly increases, which is due to the involvement of the four-photon absorption contribution. When the laser intensity is further increased (i.e. region III), the slope will gradually decrease back to a smaller value, which can be attributed to the saturated absorption. Therefore, we can conclude that up-conversion luminescence intensity enhancement using $\pi$ phase step modulation under higher laser intensity is related to the four-photon absorption contribution.

## 4. Conclusions

In conclusion, we have experimentally and theoretically demonstrated that up-conversion luminescence in a $Dy^{3+}$ ion doped glass sample can be artificially controlled by varying the $\pi$ phase step position under different laser intensities. The experimental results showed that up-conversion luminescence can be effectively suppressed but cannot be enhanced at lower laser intensity, while it can be enhanced at higher laser intensity, which indicated that the up-conversion luminescence control behavior is affected by the femtosecond laser intensity. The experimental observations can be well explained in theory by considering both the two- and four-photon absorption contributions; the relative weight of the four-photon absorption contribution in the whole excitation process will increase under the higher laser intensity, and the interference between the two- and four-photon excitation pathways will affect the up-conversion luminescence control behavior under lower and higher laser intensities. The up-conversion luminescence control of rare-earth ions under weak and intermediate femtosecond laser fields is very useful for the further application of rare-earth ions in various related areas, and can also open up a way to explore the new physical control mechanisms of up-conversion luminescence.

## Acknowledgments

This work was partly supported by Program of Introducing Talents of Discipline to Universities (B12024), National Natural Science Foundation of China (No. 51132004 and No. 11474096), Science and Technology Commission of Shanghai Municipality (No. 14JC1401500), and Higher Education Key Program of He'nan Province of China (No. 17A140025).

## References

[1] Auzel F 2004 Upconversion and anti-stokes processes with f and d ions in solids *Chem. Rev.* **104** 139–74
[2] Wang F and Liu X 2009 Recent advances in the chemistry of lanthanide-doped upconversion nanocrystals *Chem. Soc. Rev.* **38** 976–89
[3] Scheps R 1996 Upconversion laser processes *Prog. Quantum Electron.* **20** 271–358
[4] Wintner E, Sorokin E and Sorokina I T 2001 Recent developments in diode-pumped ultrashort pulse solide-state lasers *Laser. Phys.* **11** 1193–200 (https://www.researchgate.net/publication/234058165)
[5] Tessler N, Medvedev V, Kazes M, Kan S and Banin U 2002 Efficient near-infrared polymer nanocrystal light-emitting diodes *Science* **295** 1506–8
[6] Zhou P, Wang X, Ma Y, Lü H and Liu Z 2012 Review on recent progress on mid-infrared fiber lasers *Laser. Phys.* **22** 1744–51
[7] Sivakumar S, van Veggel F C J M and Raudsepp M 2005 Bright white light through up-conversion of a single NIR source from sol-gel-derived thin film made with $Ln^{3+}$-doped $LaF_3$ nanoparticles *J. Am. Chem. Soc.* **127** 12464–5
[8] Wang H-Q, Batentschuk M, Osvet A, Pinna L and Brabec C J 2011 Rare-earth ion doped up-conversion materials for photovoltaic applications *Adv. Mater.* **23** 2675–80
[9] Downing E, Hesselink L, Ralston J and Macfarlane R 1996 A three-color, solid-state, three-dimensional display *Science* **273** 1185–9
[10] Li Y, Zhang J, Luo Y, Zhang X and Hao Z 2011 Color control and white light generation of upconversion luminescence by operating dopant concentrations and pump densities in $Yb^{3+}$, $Er^{3+}$ and $Tm^{3+}$ tri-doped $Lu_2O_3$ nanocrystals *J. Mater. Chem.* **21** 2895–900
[11] Nyk M, Kumar R, Ohulchanskyy T Y, Bergey E J and Prasad P N 2008 High contrast *in vitro* and *in vivo* photoluminescence bioimaging using near infrared to near infrared up-conversion in $Tm^{3+}$ and $Yb^{3+}$ doped fluoride nanophosphors *Nano Lett.* **8** 3834–8
[12] Wang F, Tan W B, Zhang Y, Fan X and Wang M 2006 Luminescent nanomaterials for biological labelling *Nanotechnology* **17** R1–13
[13] Yu M, Li F, Chen Z, Hu H, Zhan C, Yang H and Huang C 2009 Laser scanning up-conversion luminescence microscopy for imaging cells labeled with rare-earth nanophosphors *Anal. Chem.* **81** 930–5
[14] Vetrone F, Naccache R, Zamarron A, de la Fuente A J, Sanz-Rodriguez F, Maestro L M, Rodriguez E M, Jaque D, Sole J G and Capobianco J A 2010 Temperature sensing using fluorescent nanothermometers *ACS Nano* **4** 3254–8
[15] Gai S, Li C, Yang P and Lin J 2014 Recent progress in rare earth micro/nanocrystals: soft chemical synthesis, luminescent properties, and biomedical applications *Chem. Rev.* **114** 2343–89
[16] Bai G, Tsang M K and Hao J 2015 Tuning the luminescence of phosphors: beyond conventional chemical method *Adv. Opt. Mater.* **3** 431–62
[17] Wang F and Liu X 2008 Upconversion multicolor fine-tuning: visible to near-infrared emission from lanthanide-doped $NaYF_4$ nanoparticles *J. Am. Chem. Soc.* **130** 5642–3
[18] Teng X *et al* 2012 Lanthanide-doped $Na_xScF_{3+x}$ nanocrystals: crystal structure evolution and multicolor tuning *J. Am. Chem. Soc.* **134** 8340–3
[19] Yuan D, Tan M C, Riman R E and Chow G M 2013 Comprehensive study on the size effects of the optical properties of $NaYF_4$:Yb, Er nanocrystals *J. Phys. Chem.* C **117** 13297–304
[20] Yuan D, Yi G S and Chow G M 2009 Effects of size and surface on luminescence properties of submicron upconversion $NaYF_4$: Yb, Er particles *J. Mater. Res.* **24** 2042–50
[21] Tian X, Wu Z, Jia Y, Chen J, Zheng R K, Zhang Y and Luo H 2013 Remanent-polarization-induced enhancement of photoluminescence in $Pr^{3+}$-doped lead-free ferroelectric $(Bi_{0.5}Na_{0.5})$ $TiO_3$ ceramic *Appl. Phys. Lett.* **102** 42907
[22] Tikhomirov V K, Chibotaru L F, Saurel D, Gredin P, Mortier M and Moshchalkov V V 2009 $Er^{3+}$-doped nanoparticles for optical detection of magnetic field *Nano Lett.* **9** 721–4
[23] Schietinger S, Aichele T, Wang H-Q, Nann T and Benson O 2009 Plasmon-enhanced upconversion in single $NaYF_4$:$Yb^{3+}$/$Er^{3+}$ codoped nanocrystals *Nano Lett.* **10** 134–8
[24] Brites C D S, Lima P P, Silva N J O, Millán A, Amaral V S, Palacio F and Carlos L D 2010 A luminescent molecular thermometer for long-term absolute temperature measurements at the nanoscale *Adv. Mater.* **22** 4499–504
[25] Zhou J, Deng J, Zhu H, Chen X, Teng Y, Jia H, Xu S and Qiu J 2013 Up-conversion luminescence in $LaF_3$:$Ho^{3+}$ via two-wavelength excitation for use in solar cells *J. Mater. Chem.* C **1** 8023–7
[26] Deng R, Qin F, Chen R, Huang W, Hong M and Liu X 2015 Temporal full-colour tuning through non-steady-state upconversion *Nat. Nanotechnol.* **10** 237–42
[27] Gainer C F, Joshua G S, De Silva C R and Romanowski M 2011 Control of green and red upconversion in

$NaYF_4$:$Yb^{3+}$,$Er^{3+}$ nanoparticles by excitation modulation *J. Mater. Chem.* **21** 18530–3

[28] Zhang S, Xu S, Ding J, Lu C, Jia T, Qiu J and Sun Z 2014 Single and two-photon fluorescence control of $Er^{3+}$ ions by phase-shaped femtosecond laser pulse *Appl. Phys. Lett.* **104** 14101

[29] Zhang S, Lu C, Jia T, Qiu J and Sun Z 2013 Coherent phase control of resonance-mediated two-photon absorption in rare-earth ions *Appl. Phys. Lett.* **103** 194104

[30] Yao Y, Zhang S, Zhang H, Ding J, Jia T, Qiu J and Sun Z 2014 Laser polarization and phase control of up-conversion fluorescence in rare-earth ions *Sci. Rep.* **4** 07295

[31] Zhang H, Yao Y, Zhang S, Lu C and Sun Z 2015 Up-conversion luminescence polarization control in $Er^{3+}$-doped $NaYF_4$ nanocrystals *Chin. Phys.* B **25** 23201

[32] Zhang S, Yao Y, Xu S, Liu P, Ding J, Jia T, Qiu J and Sun Z 2015 Realizing up-conversion fluorescence tuning in lanthanide-doped nanocrystals by femtosecond pulse shaping method *Sci. Rep.* **5** 13337

[33] Dudovich N, Dayan B, Faeder S M G and Silberberg Y 2001 Transform-limited pulses are not optimal for resonant multiphoton transitions *Phys. Rev. Lett.* **86** 47–50

[34] Zhang S, Zhang H, Jia T, Wang Z and Sun Z 2009 Coherent control of two-photon transitions in a two-level system with broadband absorption *Phys. Rev.* A **80** 043402

[35] Lozovoy V V, Pastirk I, Walowicz K A and Dantus M 2003 Multiphoton intrapulse interference. II. Control of two-and three-photon laser induced fluorescence with shaped pulses *J. Chem. Phys.* **118** 3187–96

[36] Walowicz K A, Pastirk I, Lozovoy V V and Dantus M 2002 Multiphoton intrapulse interference. 1. Control of multiphoton processes in condensed phases *J. Phys. Chem.* A **106** 9369–73

[37] Chuntonov L, Rybak L, Gandman A and Amitay Z 2008 Frequency-domain coherent control of femtosecond two-photon absorption: intermediate-field versus weak-field regime *J. Phys. B: At. Mol. Opt. Phys.* **41** 35504

[38] Chuntonov L, Rybak L, Gandman A and Amitay Z 2008 Enhancement of intermediate-field two-photon absorption by rationally shaped femtosecond pulses *Phys. Rev.* A **77** 021403

[39] Chuntonov L, Rybak L, Gandman A and Amitay Z 2010 Intermediate-field two-photon absorption enhancement by shaped femtosecond pulses: tolerance to phase deviation from perfect antisymmetry *Phys. Rev.* A **81** 045401